

1 **Biogenesis of type V pili**

2 Running title: Mechanism of type V pili

3 Mikio Shoji<sup>1</sup>, Satoshi Shibata<sup>2</sup>, Takayuki Sueyoshi<sup>1</sup>, Mariko Naito<sup>1</sup>, Koji Nakayama<sup>1</sup>

4

5 <sup>1</sup>Department of Microbiology and Oral Infection, Graduate School of Biomedical  
6 Sciences, Nagasaki University, Nagasaki, Nagasaki 852-8588, Japan.

7 <sup>2</sup>Molecular Cryo-Electron Microscopy Unit, Okinawa Institute of Science and  
8 Technology Graduate University, Onna, Okinawa 904-0495, Japan.


9

10 **Corresponding author**

11 Mikio Shoji, Department of Microbiology and Oral Infection, Graduate School of  
12 Biomedical Sciences, Nagasaki University, Nagasaki, Nagasaki 852-8588, Japan.

13 Email: [m-shoji@nagasaki-u.ac.jp](mailto:m-shoji@nagasaki-u.ac.jp)

14 Telephone: +81-90-819-7649

15 ORCID ID:  <https://orcid.org/0000-0002-7605-4721>

16 **Subject section and specified field**

17 Bacteriology and bacterial components

18 **Funding Statement**

19 Japan Society for the Promotion of Science, Grant/Award Numbers: 19K10072, 19K10083

20

21

22

23

24

25

26 **Abstract**

27

28 Pili or fimbriae, which are filamentous structures present on the surface of bacteria, were  
29 purified from a periodontal pathogen, *Porphyromonas gingivalis*, in 1980s. The protein  
30 component of pili (stalk pilin), which is its major component, was named FimA; it has a  
31 molecular weight of approximately 41 kDa. Since the molecular weight of the pilin is  
32 twice that of pilins from other bacterial pili, the *P. gingivalis* Fim pili were suggested to  
33 be formed via a novel mechanism. In earlier studies, we reported that the FimA pilin is  
34 secreted on the cell surface as a lipoprotein precursor, and the subsequent N-terminal  
35 processing of the FimA precursor by arginine-specific proteases is necessary for Fim pili  
36 formation. The crystal structures of FimA and its related proteins were determined  
37 recently, which show that Fim pili are formed by a protease-mediated strand-exchange  
38 mechanism. The most recent study conducted by us, wherein we performed cryo-electron  
39 microscopy of the pilus structure, provided evidence in support of this mechanism. As the  
40 *P. gingivalis* Fim pili are formed through novel transport and assembly mechanisms, such  
41 pili are now designated as type V pili. Surface lipoproteins, including the anchor pilin  
42 FimB of Fim pili that are present on the outer membrane, have been detected in certain  
43 gram-negative bacteria. Here, we describe the assembly mechanisms of pili, including

44 those of type V and other pili, as well as the lipoprotein transport mechanisms.

45

46 Key words: Bacterial components, Lipoprotein, Periodontal pathogen, Pili

47

48

49

50

51 **1. INTRODUCTION**

52

53 Periodontal disease and dental caries are two leading causes of the loss of teeth  
54 worldwide. Periodontal disease is more commonly known to cause the loss of teeth than  
55 dental caries in people aged 40 years or above in Japan<sup>1</sup>. With age progression, the  
56 proportion of people with severe symptoms of periodontal disease increases as well and  
57 this tendency is noted approximately till individuals reach 80 years of age<sup>2-3</sup>. Chronic  
58 periodontitis is known to be caused by multiple bacteria that inhabit the periodontal  
59 pocket and owing to the consequent immune responses<sup>4</sup>. Large-scale epidemiological  
60 studies have revealed the bacteria involved in the prevalence of periodontal disease<sup>5-7</sup>.  
61 . Among periodontopathic bacteria, *Porphyromonas gingivalis*, *Tannerella forsythia*, and  
62 *Treponema denticola* are strongly associated with the onset and progression of chronic  
63 periodontitis and are referred to as the “red complex”<sup>8</sup>. In particular, *P. gingivalis* is a  
64 keystone pathogen because even a small population of the pathogen can initiate and  
65 exacerbate chronic periodontitis<sup>9</sup>. Recently, a dysbiotic microbial community formed as  
66 a result of *P. gingivalis* infection was reported to mediate periodontitis in a mouse model<sup>10</sup>.

67         As *P. gingivalis* is unable to use carbohydrates as an energy source, the bacterium  
68 secrete proteases with significant proteolytic ability to use peptides/amino acids as an

69 energy source, such as gingipains, and various peptidases, including dipeptidyl peptidases,  
70 to survive in the periodontal pocket where is deeper space around teeth led by periodontal  
71 disease. Gingipains consist of arginine-specific proteases (RgpA and RgpB) and a lysine-  
72 specific protease (Kgp). These are C25 family cysteine proteases and degrade or process  
73 host matrix proteins<sup>11</sup>, immunoglobulins<sup>12</sup>, and complement factors<sup>13</sup>, as well as bacterial  
74 surface proteins, including pilins (or fimbrillins) such as FimA and Mfa1 proteins that are  
75 major subunits of Fim and Mfa pili (or fimbriae), respectively<sup>14-16</sup>.

76 *P. gingivalis* forms colonies with black pigmentation on blood agar plates. The  
77 black pigmentation is attributed to the accumulation of  $\mu$ -oxo-bis heme on the cell  
78 surface<sup>17</sup>. In particular, Kgp participates in the degradation of hemoglobin, which contains  
79 heme molecules, and accordingly, *kgp* mutants form unpigmented colonies on blood agar  
80 plates<sup>18-20</sup>. Using colony pigmentation, we discovered a type IX secretion system (T9SS)  
81 that mediates the secretion of gingipains<sup>21-27</sup> and also determined the mechanism by  
82 which gingipains attach to the cell surface, which involves binding with anionic  
83 polysaccharide containing LPS (A-LPS)<sup>28-33</sup>. In *P. gingivalis*, the gingipains-A-LPS-pili  
84 triad interacts with one another and is a major contributor to the pathogenicity of the  
85 bacteria<sup>34</sup>.

86 Bacterial pili play roles in adherence to host cells or coaggregation with other

87 bacterial cells. There are two types of pili with distinct functions: adhesive pili and sex  
88 pili; the latter is involved in the transfer of plasmid DNA from donor cells to recipient  
89 cells in conjugation. Among adhesive pili, chaperone-usher pili, curli, and type IV pili in  
90 gram-negative bacteria and sortase-dependent pili in gram-positive bacteria were reported  
91 before the discovery of type V pili<sup>35-36</sup>. Most recently, *P. gingivalis* pili were classified as  
92 a novel type of adhesive pili and designated as type V pili<sup>37</sup>. The genome of gut  
93 commensal bacteria such as *Bacteroides* spp. and *Prevotella* spp. comprises type V pili-  
94 related genes. Although there are several aspects of type V pili that remain unknown, we  
95 discuss recent findings pertaining to the biogenesis and structure of type V pili compared  
96 to those of other types of pili. In addition, bacterial lipoproteins are also discussed, as  
97 most pilins that form type V pili are secreted as lipoproteins.

98

## 99 **2 | PREVIOUSLY CHARACTERIZED BACTERIAL PILI**

100

### 101 **2.1 | Chaperone-usher pili**

102 Bacteria in Enterobacteriaceae such as *Salmonella* spp. and *Escherichia* spp. produce a  
103 variety of adhesive pili, including chaperone-usher pili<sup>38-39</sup>. Type 1 and P pili are typical  
104 chaperone-usher pili<sup>40</sup>. They consist of a linear body with 7-nm-diameter known as “rod”

105 and a thin, flexible fibril with a small tip that plays an important role in cell attachment<sup>41</sup>.  
106 Type 1 and P pili are known to be major virulence factors that mediate urinary tract  
107 infections in the bladder, urinary tract, or kidney<sup>42</sup>. Type 1 and P pili bind to  $\alpha$ -D-mannose  
108 and  $\alpha$ -D-galactopyranosyl-(1-4)- $\beta$ -D-galactopyranoside, respectively, present on the  
109 surface of urinary cells of the host. Polymerization that occurs within the usher protein is  
110 mediated by the donor-strand exchange (DSE) mechanism<sup>43</sup>. Although the major subunit  
111 protein of chaperone-usher pili contains an immunoglobulin-like fold which consists of a  
112 beta-sandwich of seven or more strands in two sheets with a Greek-key topology, it lacks  
113 the seventh  $\beta$  strand, and this leads to the formation of a hydrophobic groove. The  
114 hydrophobic groove of the subunit protein is buried by the G1 strand of chaperone protein  
115 in the periplasm, and this constitutes the donor-strand complementation (DSC)  
116 mechanism<sup>44</sup>. Subsequently, the binding partner is altered by the zip-in zip-out  
117 mechanism with the N-terminal end of the approaching protein subunit within the usher  
118 protein in the outer membrane, and this constitutes the DSE. *Escherichia coli* FimA  
119 protein of type 1 pili and PapA protein of P pili were of 18 and 20 kDa, respectively.  
120 Notably, the rod compartment of those pili possesses spring-like properties, such that  
121 bacteria with pili can adhere to urinary cells and resist urine flow<sup>35</sup>.  
122



## 123 **2.2 | Curli**

124 Curli are assembled via the nucleation precipitation pathway, which is also known as the  
125 type VIII secretion system<sup>45</sup>. Curli consist of non-branching, highly aggregative fibers  
126 and possess functional amyloid-like property which can be stained by Congo-red or  
127 Thioflavin T<sup>46</sup>. Curli consist of CsgA, CsgB, CsgC, CsgD, CsgE, CsgF, and CsgG  
128 proteins. CsgA is a major curli subunit protein and forms a substantial part of amyloid  
129 fibers. CsgB serves as a nucleator that nucleates CsgA subunits to form amyloid fibers.  
130 CsgA and CsgB are structurally similar and both consist of three components: a signal  
131 peptide, an N-terminal segment, and a C-terminal amyloid core domain comprising five  
132 repeating units. CsgC is present in the periplasm and acts as an inhibitor to prevent  
133 naturally forming CsgA polymers. CsgD, which plays a part in the *csgDEFG* operon,  
134 regulates the expression of the *csgBAC* operon. Lipoprotein CsgG forms a nonameric  
135 channel in the outer membrane and transports CsgB and CsgA from the periplasm to the  
136 cell surface. CsgE binds to CsgG in the periplasm<sup>47</sup>, while CsgF binds to the inner surface  
137 of the CsgG channel<sup>48</sup>. Initially, CsgB interacts with CsgF at the outer membrane and  
138 serves as a nucleator for the CsgA subunits. Subsequently, a secreted soluble CsgA protein  
139 binds to CsgB, self-assembles, and is eventually converted to an amyloid structure. CsgE  
140 captures CsgA and pushes it into the periplasmic chamber of CsgG to enhance its

141 translocation efficiency. The soluble CsgB and CsgA proteins usually adopt a diffusion-  
142 based, entropy-driven transport mechanism in the CsgG channel<sup>47</sup>.

143

### 144 **2.3 | Type IV pili**

145 Type IV pili are widely detected in gram-negative, and gram-positive bacteria, and in  
146 archaea; these participate in adhesion, twitching motility, swimming motility, natural  
147 competence for DNA uptake, and phage secretion<sup>49-51</sup>. Type IV pili include Type IVa,  
148 Type IVb, Tad/Flp, and Com pili, and archaeal flagellum (archaellum). Type IVa pili are  
149 the best type IV pili characterized thus far. In gram-negative bacteria, type IV pili  
150 assembly involves the participation of 10 to 18 distinct proteins that are located in the  
151 inner membrane, periplasm, and outer membrane<sup>52</sup>. PilA is a major subunit protein of the  
152 type IV pili; it contains a signal sequence and is translocated across the inner membrane  
153 by the Sec apparatus. The signal sequence of PilA is cleaved by a prepilin-specific signal  
154 peptidase to form the mature pilin<sup>53</sup>. The mature PilA protein has a lollipop-like structure  
155 with an N-terminal helix and a globular domain<sup>54</sup>. Pilus formation is initiated by the minor  
156 pilin complex that stabilizes the tip of pilus and provides a template for the assembly of  
157 major subunits<sup>55</sup>. Pilus elongation and retraction are mediated by PilC, and two  
158 antagonistic ATPases, PilB and PilT<sup>56-57</sup>. The structures and molecular weights of the

159 minor pilins are different from those of the major pilin. Minor pilins mediate specific  
160 functions such as DNA binding, aggregation, and adherence<sup>55</sup>.

161

## 162 **2.4 | Sortase-dependent pili**

163 Among gram-positive bacteria, *Actinomyces naeslundii*<sup>58</sup>, *Corynebacterium diphtheria*<sup>59</sup>,  
164 *Enterococcus faecalis*<sup>60</sup>, *Streptococcus agalactiae*<sup>61</sup>, *Streptococcus pneumoniae*<sup>62</sup>,  
165 *Streptococcus pyogenes*<sup>63</sup>, *Streptococcus suis*<sup>64</sup> were observed to contain pili<sup>65</sup>. Gram-  
166 positive bacterial pili are assembled through a sortase-dependent mechanism<sup>59</sup>. Sortases  
167 are cell surface-associated or -anchored enzymes that cleave the sorting signal sequence  
168 of secreted proteins and form isopeptide bonds between the secreted proteins and  
169 peptidoglycans or polypeptides. The cell wall sorting signal sequence consists of an  
170 LPXTG motif, a hydrophobic domain, and a short tail comprising positively charged  
171 residues<sup>66-67</sup>. The active site cysteine of the sortase contributes to cleavage of the amide  
172 bond between threonine and glycine of the LPXTG motif and generates a thioester  
173 intermediate. Nucleophilic attack by the amino group within the pentaglycine crossbridge  
174 of lipid II in the cell wall links the C-terminal threonine within the LPXTG motif of the  
175 cell surface protein<sup>65</sup>. Sortase is classified into classes A, B, C, and D<sup>65</sup>. Sortase-  
176 dependent pili are synthesized by class C sortases and certain class B sortases<sup>36</sup>. In

177 *Corynebacterium diphtheriae*, the formation of SpaA pili is initiated by isopeptide bond  
178 formation between threonine of SpaC (tip protein) and lysine of SpaA (shaft protein),  
179 following which consecutive SpaA molecules are linked sequentially. The elongation of  
180 the SpaA pili is terminated upon the incorporation of a SpaB (anchor protein) molecule  
181 by the house keeping class A sortase. Eventually, SpaA pili are anchored to the cell wall<sup>68</sup>.

182

### 183 **3 | TYPE V PILI**

184

#### 185 **3.1 | Biogenesis of Type V pili**

186 Genes associated with type V pili biogenesis are present in class Bacteroidia<sup>37</sup>. As *P.*  
187 *gingivalis* pili are the best studied type V pili, we describe the biogenesis and structure of  
188 *P. gingivalis* type V pili. *P. gingivalis* pili are known to be important virulence factors  
189 that mediate the coaggregation of the pathogen with other microorganisms and the  
190 colonization of host cells<sup>69</sup>. *P. gingivallis* contains two types of pili: Fim and Mfa<sup>70-73</sup>. In  
191 addition, the PGN\_1808 protein, which is overexpressed in strain ATCC 33277, can  
192 polymerize *in vivo* to form pilus-like filaments<sup>74</sup>. As the PGN\_1808 protein contains a  
193 FimA related motif and is matured by gingipain proteases, PGN\_1808 presumably  
194 belongs to Type V pili<sup>37</sup>. Notably, the PGN\_1808 polymer is detergent- and heat-labile

195 compared to Fim and Mfa pili. The role of PGN\_1808 has not been identified in detail.

196 FimA is a major subunit protein (stalk pilin) in Fim pili and the N-terminal sequence of

197 FimA purified from Fim pili begins at 47<sup>th</sup> alanine residue in the FimA amino acid

198 sequence encoded by the *fimA* gene, which is preceded by arginine at the 46<sup>th</sup> position<sup>75</sup>

199 (Fig. 1). N-terminal processing of FimA by the arginine-specific gingipain Rgp is

200 necessary for FimA polymerization because Rgp-deficient cells do not contain pili<sup>14</sup>. In

201 1990s, Mfa pili were determined to be the second type of pili. Mfa1 is the major

202 component of Mfa pili and has a molecular weight of approximately 70 kDa (67-75

203 kDa)<sup>71-73</sup>. The Mfa1 protein obtained from the membrane fraction begins with alanine

204 residue at the 50<sup>th</sup> position and is preceded by arginine at the 49<sup>th</sup> position<sup>15</sup> (Fig. 1). Both

205 N-terminal signal sequences of FimA and Mfa1 proteins have a motif resembling the

206 lipobox that is detected in those of bacterial lipoproteins (Fig. 1). The lipobox-like motif

207 consists of a cysteine residue and three peripheral amino acids. The thiol group of the

208 cysteine residue may bind to diacylglycerol. Therefore, we hypothesized that FimA and

209 Mfa1 pilins might be translocated as lipoproteins from the inner membrane to the outer

210 membrane. Treatment with globomycin, which is a signal peptidase II inhibitor, labeling

211 with palmitic acid, and site-specific substitution with amino acid methods demonstrated

212 that FimA and Mfa1 were secreted at the cell surface as lipoprotein precursors<sup>76</sup>. After

213 the N-terminal region of each pilin is cleaved by Rgp proteases, pilus polymerization  
214 occurs on the cell surface<sup>14-15, 76</sup>. FimB and Mfa2 function as anchor proteins that  
215 terminate pilus polymerization<sup>77-78</sup>. Furthermore, FimC, FimD, FimE, Mfa3, Mfa4, and  
216 Mfa5 are accessory proteins that are predicted to be located at the tips of Fim and Mfa  
217 pili<sup>79-81</sup>. Out of the accessory proteins, Mfa5 is secreted at the outer membrane by T9SS<sup>82</sup>.  
218 Other accessory proteins, as well as the stalk pilins FimA and Mfa1, are presumably  
219 secreted as lipoproteins and mature upon the cleavage of the N-terminal regions by Rgp  
220 proteases. The *fimA*, *fimB*, *fimC*, *fimD*, and *fimE* genes form a gene cluster, while the  
221 *mfa1*, *mfa2*, *mfa3*, *mfa4*, and *mfa5* genes form a separate gene cluster. These two gene  
222 clusters are located at different positions in the *P. gingivalis* chromosome<sup>83-84</sup>.

223 To elucidate the mechanism underlying pilus polymerization, we determined the  
224 crystal structures of 20 pili-related proteins in class Bacteroidia<sup>37</sup>. The 20 pilin related  
225 proteins belong to three Pfam families: P\_gingi\_FimA family (PF03621) which include  
226 structural (e.g., FimA and Mfa1) and tip (e.g., Mfa4) pilins, Mfa2 family (PF08842)  
227 which include anchor proteins such as FimB and Mfa2, and DUF3988 family (PF13149)  
228 whose members contain a domain of unknown function and this family is related to the  
229 other two Pfam families. The FimA protein (FimA4) from *P. gingivalis* strain W83  
230 consists of two domains, the N-terminal and C-terminal domains. Each domain comprises

231 seven  $\beta$ -strands (A1-A7 and B1-B7, respectively). Notably, an additional typical  $\beta$ -strand  
232 structure (A1'-A2') is present at the C-terminus. In several cases, the additional C-terminal  
233  $\beta$ -strands were bent inward and were closed by a loop containing an N-terminal Rgp  
234 cleavage site. Conversely, additional C-terminal  $\beta$ -strands of certain pili-related proteins  
235 which were in Mfa2 and DUF3988 families were outside. These findings suggest that  
236 Rgp proteases degrade the loop after the N-terminal A1  $\beta$ -strand to release the additional  
237 C-terminal  $\beta$ -strands, which leads to the formation of a mature form with a hydrophobic  
238 groove, and later, outward  $\beta$ -strands of the approaching mature FimA proteins embed into  
239 the groove of the former acceptor mature FimA protein, which results in pilus  
240 polymerization. To confirm that the outward C-terminal  $\beta$ -strands are embedded in the  
241 groove, we performed a Cys-Cys cross-linking analysis and observed that the C-terminal  
242  $\beta$ -strands act as a linker for polymerization<sup>37</sup>. In addition, the C-terminal  $\beta$ -strands of the  
243 anchor proteins FimB and Mfa2 play a role in determining the length of Fim and Mfa pili  
244 because the anchor pilins do not possess an N-terminal Rgp cleavage site and are  
245 lipoproteins that remain attached to the cell surface. Since the mechanisms underlying the  
246 secretion and pilus formation of *P. gingivalis* Fim and Mfa pili are different from those of  
247 previously discovered pili, we designated these pili as type V pili<sup>37</sup>. The main reasons for  
248 the newly defined type V pili are that FimA and Mfa1 are not homologous to other pili

249 proteins at the amino acid level and that they are secreted to the cell surface via a  
250 lipoprotein transport system. The crystal structures of Mfa1, Mfa2, Mfa3, and Mfa4 have  
251 been determined<sup>85-86</sup>. Similar to FimA and FimB, Mfa1 and Mfa2 contain additional C-  
252 terminal  $\beta$  strands that function as linkers. In contrast, Mfa3 and Mfa4 do not contain  
253 additional C-terminal  $\beta$  strands. Although both Mfa3 and Mfa4 proteins appear to be  
254 located at the tip, the exact binding mechanism between these proteins and the major pilin  
255 Mfa1 remains unknown. C-terminal peptides of Mfa1 and FimA inhibit the  
256 polymerization of Mfa1 and FimA proteins, respectively<sup>87</sup>. The construction of more  
257 effective inhibitors of pilus formation that are based on the recently discovered crystal  
258 structures of Fim-related proteins will help prevent the colonization by the periodontal  
259 pathogen.

260           Recently, we determined the crystal structures of FimA proteins: FimA1 from  
261 strain ATCC 33277 and FimA2 from strain TDC60. The proteins from both strains consist  
262 of two domains, the N-terminal and C-terminal domains with an additional typical  $\beta$ -  
263 strand structure (A1') at the C-terminus<sup>88</sup> (Fig. 2). In addition, we successfully performed  
264 the *in vitro* formation of the FimA polymer that is generated by mixing recombinant FimA  
265 protein purified from *E. coli* with RgpB protease isolated from *P. gingivalis*. Cryo-  
266 electron microscopic observation of the FimA polymer revealed that additional C-



267 terminal strands of FimA protein are embedded in the groove of a preceding FimA protein,  
268 which indicates the protease-mediated strand-exchange of type V pilus polymerization  
269 (Fig. 3). Immuno-electron microscopy with anti-His tag antibody revealed that the N-  
270 terminal His tag of recombinant FimA, which is separated from FimA upon cleavage by  
271 RgpB protease, is detected at one end of the FimA polymer, which suggests that the N-  
272 terminal anchor strand of FimA remains embedded in the groove even after RgpB  
273 cleavage<sup>88</sup>. We found that FimA that lack the last amino acid residue tryptophan at the  
274 383<sup>rd</sup> position (FimA[Δ383]), which cannot polymerize, is located on the cell surface. To  
275 determine whether the N-terminal anchor strand remains associated with the N-terminal  
276 domain of FimA[Δ383] post RgpB cleavage, we created FimA[Δ383] derivatives with  
277 cysteine pairs in the anchor strand and its neighboring strands after substituting intrinsic  
278 cysteines with alanines. The cross-linking of these mutants with a crosslinking agent, dithio-  
279 bis-maleimidoethane, led to an increase in the molecular mass of FimA, which corresponded  
280 to the molecular mass of the anchor strand, and this effect was reversed upon the addition of  
281 β-mercaptoethanol<sup>88</sup>. These results indicate that pilins are anchored to the cell surface even  
282 after RgpB cleavage, which facilitates a smooth reaction between pilins. We also observed  
283 that the FimA polymer can be generated using a mouse-derived arginine-specific protease  
284 instead of RgpB, which suggests that only the proteolytic function of RgpB is a

285 prerequisite for FimA polymerization (Shibata et al., unpublished data) (Fig. 4).

286

### 287 **3.2 | Lipidation of bacterial lipoproteins**

288 As FimA-related proteins such as FimA, FimB, FimC, FimD, Mfa1, Mfa2, Mfa3, and

289 Mfa4 are secreted by lipoproteins<sup>76</sup>, here, we discuss the lipoproteins present in bacteria.

290 Lipoproteins are present in bacteria, archaea, and eukarya. Lipoproteins present in gram-

291 negative and gram-positive bacteria possess a unique feature: they undergo membrane

292 association, which involves the linking of a diacylglycerol unit thioether with the N-

293 terminal cysteine of the lipoprotein<sup>89</sup>. Lipidation is mediated by prolipoprotein

294 diacylglyceryl transferase (Lgt) after translocation across the cytoplasmic membrane

295 occurs via the Sec or Tat translocation pathway. Next, the lipidated proteins are cleaved

296 by lipoprotein-specific signal peptidase II (LspA). In *E. coli*, additional fatty acids are

297 linked to the N-terminus of the LspA-processed protein by N-acyltransferase (Lnt).

298 The *lgt* and *lspA* genes are essential in gram-negative bacteria and nonessential

299 in gram-positive bacteria<sup>90-92</sup>. We also attempted to construct *P. gingivalis* mutants

300 lacking *lgt* and *lspA* genes. However, attempt has been unsuccessful thus far, which

301 suggests that these genes play vital roles in the proliferation of *P.gingivalis* (Shoji et al.,

302 unpublished data). The tri-acylation of lipoproteins is mediated by Lnt in *E. coli*. Notably,

303 lipoprotein intramolecular transacylase (Lit) in gram-positive bacteria was recently found  
304 to be a novel N-acylating enzyme<sup>93-94</sup>. PG\_1828 of *P. gingivalis* 381 was reported to be  
305 a tri-acylated lipoprotein<sup>95</sup>. However, we did not detect Lnt or Lit homologs in *P.*  
306 *gingivalis*. Further analysis is necessary to determine whether triacylated lipoproteins are  
307 common in other *P. gingivalis* strains and the enzyme responsible for N-acylation.

308

### 309 **3.3 | Lipoprotein sorting from inner membrane to outer membrane**

310 LolA, a periplasmic protein, was found to be involved in lipoprotein sorting to the outer  
311 membrane in *E. coli*<sup>96</sup>; LolB, which is located in the inner leaflet of the outer membrane,  
312 was found to act as a receiver for the LolA-carrying lipoprotein<sup>97-98</sup>. LolA homologs are  
313 present in various bacteria and more than 3,000 bacterial species contain proteins with  
314 the LolA domain, as revealed in the Pfam family database. In addition, LolA\_like  
315 (PF17131) and LolA\_2 (PF16584) family proteins were detected in 1,000 and 267  
316 bacterial species, respectively.

317 LolA has eleven antiparallel  $\beta$ -sheets and three  $\alpha$ -helices, which form an  
318 incomplete  $\beta$ -barrel structure with a lid<sup>99</sup>. The barrel has a hydrophobic cavity and can  
319 bind the acyl chains of lipoproteins. The *lolA* gene is essential in *E. coli* and *Pseudomonas*  
320 *aeruginosa*<sup>100-101</sup>, whereas it is nonessential in *Helicobacter pylori*<sup>102</sup>, *Flavobacterium*

321 *johnsoniae*<sup>103</sup>, *Cellulophaga algicola*<sup>104</sup>, or *Xanthomonas campestris* pv. *campestris*<sup>105</sup>,  
322 as evidenced by the successful generation of respective *lolA*-deficient mutants. Notably,  
323 in *E. coli*, both *lolA*- and *lolB*- deficient mutants can be generated in the genetic  
324 background with *lpp* and *rscB* mutations and the activating Cpx envelope stress  
325 response<sup>106</sup>. These results indicate the presence of an alternative LolA-independent  
326 lipoprotein-trafficking mechanism. The *P. gingivalis* genome does not encode any  
327 homologs of the LolA family (PF03548), as revealed in the Pfam database, although we  
328 detected homologs of the LolA\_2 family (PG\_1635 in strain W83; PGN\_0486 in strain  
329 ATCC 33277) and LolA\_like family (PG\_1179 in strain W83; PGN\_0947 and PGN\_1919  
330 in strain ATCC 33277). In strain ATCC 33277, PGN\_0947 and PGN\_1919 were observed  
331 to be duplicates and were located within two copies of TnPg17<sup>84</sup>. *P. gingivalis* W83 and  
332 TDC60 each contain one copy of TnPg17 at the same chromosomal position as that in  
333 PGN\_0947 in ATCC 33277. Using strain W83, we generated a mutant that lacks PG\_1179  
334 and PG\_1635 genes and found that the mutant formed colonies with black-pigmentation  
335 on blood agar plates, similar to those formed by the parental strain W83. Furthermore, the  
336 PG\_1179 and PG\_1635 double mutant of strain W83 was found to have the ability to  
337 form Fim pili, as revealed by the introduction of the *fimA* gene of ATCC 33277 into the  
338 mutant and detection of FimA ladder bands indicating FimA polymerization upon

339 immune-reaction with anti-ATCC 33277 FimA antibody (Shoji et al., unpublished data).  
340 This indicates that the FimA lipoprotein is translocated to the cell surface through a  
341 lipoprotein secretion pathway without the LolA-related proteins (Shoji et al., unpublished  
342 data). Further analysis is required to elucidate the lipoprotein trafficking mechanism in *P.*  
343 *gingivalis*.

344           The crystal structure of LolB is considerably similar to that of LolA. The C-  
345 terminal loop of LolA is its characteristic trait and can help avoid retrograde localization  
346 of lipoproteins to the inner membrane<sup>107</sup>. Conversely, leucine at the 68<sup>th</sup> position present  
347 in the protruding loop of LolB plays an important role in outer membrane targeting<sup>108</sup>.  
348 LolA (Pfam code PF03548) is particularly conserved in phyla Proteobacteria, and  
349 Bacteroidetes, whereas LolB (Pfam code PF03550) is conserved only in phylum  
350 Proteobacteria<sup>109</sup>. *P. gingivalis* and *Bacteroidetes* spp., among other bacteria from phylum  
351 Bacteroidetes lack LolB homologs, which suggests that the function executed by LolB  
352 are not necessary in these bacteria, or perhaps these bacteria contain a different protein  
353 with the same function as LolB.

354           Outer membrane proteins in gram-negative bacteria are synthesized in the  
355 cytoplasm and transported across the inner membrane by the Sec apparatus. Subsequently,  
356 the signal peptide is cleaved by a signal peptidase, and the processed protein is then

357 transported by outer membrane transportation systems, such as the  $\beta$ -barrel assembly  
358 machinery (BAM) and the translocation and assembly module (TAM)<sup>110</sup>. The BAM  
359 complex is known to be an essential component in *E. coli*. In *P. gingivalis*, BamA  
360 (PGN\_0299) and BamD (PGN\_1354) are thought to form the Bam complex. The *P.*  
361 *gingivalis* BamA homolog (PGN\_0299) is predicted to be an essential component of the  
362 pathogen<sup>111-112</sup>. TAM consists of TamA and TamB proteins. These proteins are assumed  
363 to transport autotransporter proteins and hydrophobic molecules<sup>113</sup>. We detected  
364 homologs of TamA (PGN\_0147 and PGN\_0973) and TamB (PGN\_0145 and PGN\_0148)  
365 in *P. gingivalis*. *P. gingivalis* PGN\_0147 and PGN\_0973 double mutant formed colonies  
366 with black-pigmentation on blood agar plates, and yet, expressed Fim and Mfa pili, which  
367 suggests that TamA homologs are not involved in lipoprotein transport in the organism  
368 (Shoji et al., unpublished data).

369

### 370 **3.4 | Lipoprotein transport to the cell surface**

371 In gram-negative bacteria, lipoproteins are known to have the following features: (i)  
372 diacylglyceration at a cysteine residue that is located at the end of the N-terminal signal  
373 sequence by the diacylglyceryl transferase, Lgt, (ii) cleavage of the N-terminal signal  
374 sequence by the type II signal peptidase, Lsp, in the inner membrane, and (iii) addition of

375 an N-acyl fatty acid to the N-terminal end of the protein by the N-acyltransferase, Lnt, in  
376 the inner membrane. The lipoprotein sorting systems in *E. coli* are well studied<sup>114</sup>. *E. coli*  
377 lipoproteins are translocated from the outer leaflet of the inner membrane to the inner  
378 leaflet of the outer membrane by the lipoprotein sorting machinery, which consists of a  
379 lipoprotein-specific ABC transporter, the LolCDE complex in the inner membrane, and  
380 aforementioned LolA and LolB proteins. Some lipoproteins remain in the inner  
381 membrane because they possess the Lol avoidance signal that has asparagine and  
382 glutamic acid residues in the second (+2) and third (+3) positions after lipidated cysteine.  
383 *E. coli* has more than 90 lipoproteins. Among them, only RcsF<sup>115</sup> and Pal<sup>116</sup> proteins are  
384 translocated to the outer leaflet of the outer membrane.

385           Conversely, it is noteworthy that *Borrelia burgdorferi* expresses more than 80  
386 lipoproteins on its cell surface<sup>117-118</sup>. However, molecules that translocate lipoproteins  
387 across the outer membrane, such as flippase, have not been detected. Zückert's group  
388 found that the surface lipoproteins contain tether regions that are necessary for  
389 translocation across the outer membrane, which consist of lipidated cysteine and nearly  
390 ten amino acids; however, there are no specific consensus amino acids in the tether  
391 regions<sup>119-121</sup>. *Bacteroides* spp. contain starch-degrading surface lipoproteins such as  
392 SusC, SusD, SusE, SusF, and SusG<sup>122-124</sup>. Lauber et al<sup>125</sup> observed that the surface

393 lipoproteins of *Bacteroides* harbor lipidated cysteine with XQKDDE as a consensus motif  
394 for translocation across the outer membrane. The consensus motif is named the  
395 lipoprotein export sequence (LES). The presence of acidic residues such as aspartic acid  
396 and glutamic acid in the LES are particularly important for translocation across the outer  
397 membrane. LES-like motifs are present in the surface lipoproteins of other bacteria such  
398 as *Capnocytophaga canimorsus*, *Flavobacterium johnsoniae*, and *Bacteroides fragilis*.  
399 As mentioned above, *P. gingivalis* FimA and Mfa1, the major stalk pilins of Fim and Mfa  
400 pili, respectively, are positioned at the cell surface as lipoproteins before the N-terminal  
401 regions of the proteins are cleaved by Rgp proteases<sup>76</sup>. Anchor and accessory pilins of  
402 Fim and Mfa, except Mfa5<sup>82</sup>, are also secreted as lipoproteins. Fim and Mfa pilins, except  
403 Mfa5, contain LES-like sequences in the N-terminal regions. Fim- and Mfa-related  
404 proteins are widely conserved in *Bacteroides* spp<sup>37</sup>. Our preliminary survey on  
405 lipoproteins using LIPO<sup>126</sup> and Lipo P1.0<sup>127</sup> programs revealed that there are 85  
406 lipoproteins in *P. gingivalis*. Of these, 67 lipoproteins were predicted by both programs.  
407 Besides the Fim and Mfa proteins, the SusD homolog RagB, IhtB, HmuY, and Omp28  
408 were predicted to be present as surface lipoproteins in *P. gingivalis*. The lipoproteins are  
409 likely to have an LES because acidic residues are positioned adjacent to cysteine. The  
410 T9SS component proteins, PorK, PorE, and PorW are predicted to be lipoproteins. PorK



411 is located in the inner leaflet of the outer membrane<sup>128</sup>, while the subcellular positions of  
412 PorE and PorW have not been determined. As PorE, PorW, and PorK do not contain LES-  
413 like sequences, it is assumed that these are not positioned at the cell surface (Fig. 5).

414           Notably, Hooda et al.<sup>129</sup> found that an outer membrane protein, Slam, can  
415 translocate lipoproteins to the cell surface in *Neisseria* spp. Slam possesses an N-terminal  
416 domain that contains tetratricopeptide repeats and a C-terminal  $\beta$ -barrel domain named  
417 DUF560. Slam homologs are present in bacterial species that inhabit in diverse  
418 environments, including free-living, commensal, and pathogenic bacteria such as *N.*  
419 *meningitidis*, *Vibrio cholerae*, *Salmonella enterica*, and *Acinetobacter baumannii*;  
420 however, Slam homologs are absent in *Borrelia* spp., *Bacteroides* spp.<sup>130</sup>, and *P.*  
421 *gingivalis*.

422

#### 423 **4 | CONCLUDING REMARKS**

424

425 *P. gingivalis* is known to be a keystone pathogen that induces the onset and exacerbation  
426 of periodontal disease. Inclusion of *P. gingivalis* in the periodontal microbiota that  
427 constitutes the periodontal biofilm alters the normal state of the periodontal environment  
428 to a periodontopathic state. Therefore, it is necessary to develop pharmaceutical drugs

429 targeting *P. gingivalis*. Drugs that control pilin transport or pilus formation in the  
430 bacterium are likely to be good candidates, since such drugs can specifically eliminate  
431 the bacterium from the periodontal environment without affecting the normal microbiota  
432 and are distinctly different from previously known antibiotics.

433

434

435

436 **Acknowledgements**

437 We thank Editage ([www.editage.com](http://www.editage.com)) for English language editing.

438

439 **Disclosure**

440 There is no conflict of interest.

441

442 **Data Availability Statement**

443 Data available on request due to privacy/ethical restrictions.

444 **References**

- 445 1. 8020zaidan. The second national survey on the reasons for extraction of permanent  
446 teeth, 2018
- 447 2. Nazir M. A. Prevalence of periodontal disease, its association with systemic  
448 diseases and prevention. *International journal of health sciences*, 2017; 11(2), 72–  
449 80.
- 450 3. Tonetti MS, Bottenberg P, Conrads G, et al. Dental caries and periodontal diseases  
451 in the ageing population: call to action to protect and enhance oral health and well-  
452 being as an essential component of healthy ageing - Consensus report of group 4 of  
453 the joint EFP/ORCA workshop on the boundaries between caries and periodontal  
454 diseases. *J Clin Periodontol*. 2017;44 Suppl 18:S135-S144. doi:10.1111/jcpe.12681
- 455 4. Könönen E, GURSOY M, GURSOY UK. Periodontitis: A Multifaceted Disease of  
456 Tooth-Supporting Tissues. *J Clin Med*. 2019;8(8):1135. Published 2019 Jul 31.  
457 doi:10.3390/jcm8081135
- 458 5. Rodenburg JP, van Winkelhoff AJ, Winkel EG, Goené RJ, Abbas F, de Graff J.  
459 Occurrence of *Bacteroides gingivalis*, *Bacteroides intermedius* and *Actinobacillus*  
460 *actinomycetemcomitans* in severe periodontitis in relation to age and treatment

- 461 history. *J Clin Periodontol*. 1990;17(6):392–399. doi:10.1111/j.1600-  
462 051x.1990.tb00036.x
- 463 6. Slots J, Feik D, Rams TE. *Actinobacillus actinomycetemcomitans* and *Bacteroides*  
464 *intermedius* in human periodontitis: age relationship and mutual association. *J Clin*  
465 *Periodontol*. 1990;17(9):659–662.
- 466 7. Chigasaki O, Takeuchi Y, Aoki A, et al. A cross-sectional study on the  
467 periodontal status and prevalence of red complex periodontal pathogens in a  
468 Japanese population. *J Oral Sci*. 2018;60(2):293–303. doi:10.2334/josnusd.17-  
469 0223
- 470 8. Holt SC, Ebersole JL. *Porphyromonas gingivalis*, *Treponema denticola*, and  
471 *Tannerella forsythia*: the "red complex", a prototype polybacterial pathogenic  
472 consortium in periodontitis. *Periodontol 2000*. 2005;38:72–122.  
473 doi:10.1111/j.1600-0757.2005.00113.x
- 474 9. Hajishengallis G, Liang S, Payne MA, et al. Low-abundance biofilm species  
475 orchestrates inflammatory periodontal disease through the commensal microbiota  
476 and complement. *Cell Host Microbe*. 2011;10(5):497–506.  
477 doi:10.1016/j.chom.2011.10.006
- 478 10. Payne MA, Hashim A, Alsam A, et al. Horizontal and vertical transfer of oral

- 479 microbial dysbiosis and periodontal disease. *J Dent Res.* 2019;98(13):1503–1510.  
480 doi:10.1177/0022034519877150
- 481 11. Potempa J, Banbula A, Travis J. Role of bacterial proteinases in matrix  
482 destruction and modulation of host responses. *Periodontol 2000.* 2000;24:153–  
483 192. doi:10.1034/j.1600-0757.2000.2240108.x
- 484 12. Fujimura S, Hirai K, Shibata Y, Nakayama K, Nakamura T. Comparative  
485 properties of envelope-associated arginine-gingipains and lysine-gingipain of  
486 *Porphyromonas gingivalis*. *FEMS Microbiol Lett.* 1998;163(2):173–179.  
487 doi:10.1111/j.1574-6968.1998.tb13042.x
- 488 13. Wingrove JA, DiScipio RG, Chen Z, Potempa J, Travis J, Hugli TE. Activation of  
489 complement components C3 and C5 by a cysteine proteinase (gingipain-1) from  
490 *Porphyromonas (Bacteroides) gingivalis*. *J Biol Chem.* 1992;267(26):18902–  
491 18907.
- 492 14. Nakayama K, Yoshimura F, Kadowaki T, Yamamoto K. Involvement of arginine-  
493 specific cysteine proteinase (Arg-gingipain) in fimbriation of *Porphyromonas*  
494 *gingivalis*. *J Bacteriol.* 1996;178(10):2818–2824. doi:10.1128/jb.178.10.2818-  
495 2824.

- 496 15. Kadowaki T, Nakayama K, Yoshimura F, Okamoto K, Abe N, Yamamoto K.  
497 Arg-gingipain acts as a major processing enzyme for various cell surface proteins  
498 in *Porphyromonas gingivalis*. *J Biol Chem*. 1998;273(44):29072–29076.  
499 doi:10.1074/jbc.273.44.29072
- 500 16. Haruyama K, Yoshimura A, Naito M, Kishimoto M, Shoji M, Abiko Y, Hara Y,  
501 and Nakayama K: Identification of a gingipain-sensitive surface ligand of  
502 *Porphyromonas gingivalis* that induces TLR2- and TLR4-independent NF-κB  
503 activation in CHO cells. *Infect. Immun*. 2009;77(10):4414-4420.
- 504 17. Smalley JW, Silver J, Marsh PJ, Birss AJ. The periodontopathogen  
505 *Porphyromonas gingivalis* binds iron protoporphyrin IX in the mu-oxo dimeric  
506 form: an oxidative buffer and possible pathogenic mechanism. *Biochem J*.  
507 1998;331 (Pt 3):681–685. doi:10.1042/bj3310681
- 508 18. Okamoto K, Nakayama K, Kadowaki T, Abe N, Ratnayake DB, Yamamoto K.  
509 Involvement of a lysine-specific cysteine proteinase in hemoglobin adsorption and  
510 heme accumulation by *Porphyromonas gingivalis*. *J Biol Chem*.  
511 1998;273(33):21225–21231. doi:10.1074/jbc.273.33.21225
- 512 19. Lewis JP, Dawson JA, Hannis JC, Muddiman D, Macrina FL. Hemoglobinase  
513 activity of the lysine gingipain protease (Kgp) of *Porphyromonas gingivalis* W83.

- 514 *J Bacteriol.* 1999;181(16):4905–4913.
- 515 20. Curtis MA, Aduse Opoku J, Rangarajan M, et al. Attenuation of the virulence of  
516 *Porphyromonas gingivalis* by using a specific synthetic Kgp protease inhibitor.  
517 *Infect Immun.* 2002;70(12):6968–6975. doi:10.1128/iai.70.12.6968-6975.2002
- 518 21. Sato K, Sakai E, Veith PD, et al. Identification of a new membrane-associated  
519 protein that influences transport/maturation of gingipains and adhesins of  
520 *Porphyromonas gingivalis*. *J Biol Chem.* 2005;280(10):8668–8677.  
521 doi:10.1074/jbc.M413544200
- 522 22. Sato K, Naito M, Yukitake H, et al. A protein secretion system linked to  
523 bacteroidete gliding motility and pathogenesis. *Proc Natl Acad Sci U S A.*  
524 2010;107(1):276–281. doi:10.1073/pnas.0912010107
- 525 23. Shoji M, Sato K, Yukitake H, et al. Por secretion system-dependent secretion and  
526 glycosylation of *Porphyromonas gingivalis* hemin-binding protein 35. *PLoS One.*  
527 2011;6(6):e21372. doi:10.1371/journal.pone.0021372
- 528 24. Sato K, Yukitake H, Narita Y, Shoji M, Naito M, Nakayama K. Identification of  
529 *Porphyromonas gingivalis* proteins secreted by the Por secretion system. *FEMS*  
530 *Microbiol Lett.* 2013;338(1):68–76. doi:10.1111/1574-6968.12028
- 531 25. Nakayama K. *Porphyromonas gingivalis* and related bacteria: from colonial



532 pigmentation to the type IX secretion system and gliding motility. *J Periodontal*  
533 *Res.* 2015;50(1):1–8. doi:10.1111/jre.12255

534 26. Sato K, Kakuda S, Yukitake H, et al. Immunoglobulin-like domains of the cargo  
535 proteins are essential for protein stability during secretion by the type IX secretion  
536 system. *Mol Microbiol.* 2018;110(1):64–81. doi:10.1111/mmi.14083

537 27. Naito M, Tominaga T, Shoji M, Nakayama K. PGN\_0297 is an essential  
538 component of the type IX secretion system (T9SS) in *Porphyromonas gingivalis*:  
539 Tn-seq analysis for exhaustive identification of T9SS-related genes. *Microbiol*  
540 *Immunol.* 2019;63(1):11–20. doi:10.1111/1348-0421.12665

541 28. Curtis MA, Thickett A, Slaney JM, et al. Variable carbohydrate modifications to  
542 the catalytic chains of the RgpA and RgpB proteases of *Porphyromonas gingivalis*  
543 W50. *Infect Immun.* 1999;67(8):3816–3823.

544 29. Shoji M, Ratnayake DB, Shi Y, et al. Construction and characterization of a  
545 nonpigmented mutant of *Porphyromonas gingivalis*: cell surface polysaccharide  
546 as an anchorage for gingipains. *Microbiology.* 2002;148(Pt 4):1183–1191.  
547 doi:10.1099/00221287-148-4-1183

- 548 30. Shoji M, Yukitake H, Sato K, et al. Identification of an O-antigen chain length  
549 regulator, WzzP, in *Porphyromonas gingivalis*. *Microbiologyopen*.  
550 2013;2(3):383-401. doi:10.1002/mbo3.84
- 551 31. Shoji M, Sato K, Yukitake H, Naito M, Nakayama K. Involvement of the Wbp  
552 pathway in the biosynthesis of *Porphyromonas gingivalis* lipopolysaccharide with  
553 anionic polysaccharide. *Sci Rep*. 2014;4:5056. Published 2014 May 23.  
554 doi:10.1038/srep05056
- 555 32. Shoji M, Nakayama K. Glycobiology of the oral pathogen *Porphyromonas*  
556 *gingivalis* and related species. *Microb Pathog*. 2016;94:35–41.  
557 doi:10.1016/j.micpath.2015.09.012
- 558 33. Shoji M, Sato K, Yukitake H, et al. Identification of genes encoding  
559 glycosyltransferases involved in lipopolysaccharide synthesis in *Porphyromonas*  
560 *gingivalis*. *Mol Oral Microbiol*. 2018;33(1):68–80. doi:10.1111/omi.12200
- 561 34. Nakayama K.: The type IX secretion system and the type V pilus in the phylum  
562 *Bacteroidetes*. *Japanese Journal of Bacteriology* 72(4), 219-227, 2017
- 563 35. Hospenthal MK, Costa TRD, Waksman G. A comprehensive guide to pilus  
564 biogenesis in Gram-negative bacteria. *Nat Rev Microbiol*. 2017;15(6):365–379.  
565 doi:10.1038/nrmicro.2017.40

- 566 36. Khare B, V L Narayana S. Pilus biogenesis of Gram-positive bacteria: Roles of  
567 sortases and implications for assembly. *Protein Sci.* 2017;26(8):1458–1473.  
568 doi:10.1002/pro.3191
- 569 37. Xu Q, Shoji M, Shibata S, et al. A distinct type of pilus from the human  
570 microbiome. *Cell.* 2016;165(3):690–703. doi:10.1016/j.cell.2016.03.016
- 571 38. Busch A, Waksman G. Chaperone-usher pathways: diversity and pilus assembly  
572 mechanism. *Philos Trans R Soc Lond B Biol Sci.* 2012;367(1592):1112-1122.  
573 doi:10.1098/rstb.2011.0206
- 574 39. Hansmeier N, Miskiewicz K, Elpers L, Liss V, Hensel M, Sterzenbach T.  
575 Functional expression of the entire adhesiome of *Salmonella enterica* serotype  
576 Typhimurium. *Sci Rep.* 2017;7(1):10326. doi:10.1038/s41598-017-10598-2
- 577 40. Werneburg GT, Thanassi DG. Pili Assembled by the Chaperone/Usher Pathway in  
578 *Escherichia coli* and *Salmonella*. *EcoSal Plus.* 2018;8(1):10.  
579 doi:10.1128/ecosalplus.ESP-0007-2017
- 580 41. Kuehn MJ, Heuser J, Normark S, Hultgren SJ. P pili in uropathogenic *E. coli* are  
581 composite fibres with distinct fibrillar adhesive tips. *Nature.* 1992;356(6366):252-  
582 255. doi:10.1038/356252a0
- 583 42. Mizunoe Y, Wai SN. Bacterial fimbriae in the pathogenesis of urinary tract

- 584 infection. *J Infect Chemother*. 1998;4, 1–5. <https://doi.org/10.1007/BF02490057>
- 585 43. Phan G, Remaut H, Wang T, et al. Crystal structure of the FimD usher bound to its  
586 cognate FimC-FimH substrate. *Nature*. 2011;474(7349):49–53.  
587 doi:10.1038/nature10109
- 588 44. Hung DL, Knight SD, Woods RM, Pinkner JS, Hultgren SJ. Molecular basis of  
589 two subfamilies of immunoglobulin-like chaperones. *EMBO J*. 1996;15(15):3792-  
590 3805.
- 591 45. Chagnot C, Zorgani MA, Astruc T, Desvaux M. Proteinaceous determinants of  
592 surface colonization in bacteria: bacterial adhesion and biofilm formation from a  
593 protein secretion perspective. *Front Microbiol*. 2013 Oct 14;4:303. doi:  
594 10.3389/fmicb.2013.00303.
- 595 46. Chapman MR, Robinson LS, Pinkner JS, et al. Role of *Escherichia coli* curli  
596 operons in directing amyloid fiber formation. *Science*. 2002;295(5556):851–855.  
597 doi:10.1126/science.1067484
- 598 47. Goyal P, Krasteva PV, Van Gerven N, et al. Structural and mechanistic insights  
599 into the bacterial amyloid secretion channel CsgG. *Nature*. 2014;516(7530):250–  
600 253. doi:10.1038/nature13768
- 601 48. Yan Z, Yin M, Chen J, Li X. Assembly and substrate recognition of curli

602 biogenesis system. *Nat Commun.* 2020;11(1):241. Published 2020 Jan 13.  
603 doi:10.1038/s41467-019-14145-7

604 49. Albers SV, Jarrell KF. The Archaeallum: An Update on the Unique Archaeal  
605 Motility Structure. *Trends Microbiol.* 2018;26(4):351-362.  
606 doi:10.1016/j.tim.2018.01.004

607 50. Craig L, Forest KT, Maier B. Type IV pili: dynamics, biophysics and functional  
608 consequences. *Nat Rev Microbiol.* 2019;17(7):429-440. doi:10.1038/s41579-019-  
609 0195-4

610 51. Pelicic V. Monoderm bacteria: the new frontier for type IV pilus biology. *Mol*  
611 *Microbiol.* 2019;112(6):1674-1683. doi:10.1111/mmi.14397

612 52. Pelicic V. Type IV pili: e pluribus unum?. *Mol Microbiol.* 2008;68(4):827–837.  
613 doi:10.1111/j.1365-2958.2008.06197.x

614 53. Strom MS, Nunn DN, Lory S. A single bifunctional enzyme, PilD, catalyzes  
615 cleavage and N-methylation of proteins belonging to the type IV pilin family.  
616 *Proc Natl Acad Sci U S A.* 1993;90(6):2404–2408. doi:10.1073/pnas.90.6.2404

617 54. Giltner CL, Nguyen Y, Burrows LL. Type IV pilin proteins: versatile molecular  
618 modules. *Microbiol Mol Biol Rev.* 2012;76(4):740–772.  
619 doi:10.1128/MMBR.00035-12

- 620 55. Jacobsen T, Bardiaux B, Francetic O, Izadi-Pruneyre N, Nilges M. Structure and  
621 function of minor pilins of type IV pili [published online ahead of print, 2019 Nov  
622 29]. *Med Microbiol Immunol*. 2019;10.1007/s00430-019-00642-5.  
623 doi:10.1007/s00430-019-00642-5
- 624 56. Takhar HK, Kemp K, Kim M, Howell PL, Burrows LL. The platform protein is  
625 essential for type IV pilus biogenesis. *J Biol Chem*. 2013;288(14):9721–9728.  
626 doi:10.1074/jbc.M113.453506
- 627 57. Tsai CL, Tainer JA. The ATPase motor turns for type IV pilus assembly. *Structure*.  
628 2016;24(11):1857–1859. doi:10.1016/j.str.2016.10.002
- 629 58. Yeung MK, Donkersloot JA, Cisar JO, Ragsdale PA. Identification of a gene  
630 involved in assembly of *Actinomyces naeslundii* T14V type 2 fimbriae. *Infect*  
631 *Immun*. 1998;66(4):1482–1491.
- 632 59. Ton-That H, Schneewind O. Assembly of pili on the surface of *Corynebacterium*  
633 *diphtheriae*. *Mol Microbiol*. 2003;50(4):1429–1438. doi:10.1046/j.1365-  
634 2958.2003.03782.x
- 635 60. Nallapareddy SR, Singh KV, Sillanpää J, et al. Endocarditis and biofilm-  
636 associated pili of *Enterococcus faecalis*. *J Clin Invest*. 2006;116(10):2799–2807.  
637 doi:10.1172/JCI29021

- 638 61. Lauer P, Rinaudo CD, Soriani M, et al. Genome analysis reveals pili in Group B  
639 *Streptococcus*. *Science*. 2005;309(5731):105. doi:10.1126/science.1111563
- 640 62. Barocchi MA, Ries J, Zogaj X, et al. A pneumococcal pilus influences virulence  
641 and host inflammatory responses. *Proc Natl Acad Sci U S A*. 2006;103(8):2857–  
642 2862. doi:10.1073/pnas.0511017103
- 643 63. Mora M, Bensi G, Capo S, et al. Group A *Streptococcus* produce pilus-like  
644 structures containing protective antigens and Lancefield T antigens. *Proc Natl*  
645 *Acad Sci U S A*. 2005;102(43):15641–15646. doi:10.1073/pnas.0507808102
- 646 64. Takamatsu D, Nishino H, Ishiji T, et al. Genetic organization and preferential  
647 distribution of putative pilus gene clusters in *Streptococcus suis*. *Vet Microbiol*.  
648 2009;138(1-2):132–139. doi:10.1016/j.vetmic.2009.02.013
- 649 65. Hendrickx AP, Budzik JM, Oh SY, Schneewind O. Architects at the bacterial  
650 surface - sortases and the assembly of pili with isopeptide bonds. *Nat Rev*  
651 *Microbiol*. 2011;9(3):166–176. doi:10.1038/nrmicro2520
- 652 66. Navarre WW, Schneewind O. Proteolytic cleavage and cell wall anchoring at the  
653 LPXTG motif of surface proteins in gram-positive bacteria. *Mol Microbiol*.  
654 1994;14(1):115–121. doi:10.1111/j.1365-2958.1994.tb01271.x
- 655 67. Mazmanian SK, Ton-That H, Schneewind O. Sortase-catalysed anchoring of

- 656 surface proteins to the cell wall of *Staphylococcus aureus*. *Mol Microbiol.*  
657 2001;40(5):1049–1057. doi:10.1046/j.1365-2958.2001.02411.x
- 658 68. Mandlik A, Das A, Ton-That H. The molecular switch that activates the cell wall  
659 anchoring step of pilus assembly in gram-positive bacteria. *Proc Natl Acad Sci U*  
660 *S A.* 2008;105(37):14147–14152. doi:10.1073/pnas.0806350105
- 661 69. Amano A. Bacterial adhesins to host components in periodontitis. *Periodontol*  
662 *2000.* 2010;52(1):12–37. doi:10.1111/j.1600-0757.2009.00307.x
- 663 70. Yoshimura F, Takahashi K, Nodasaka Y, Suzuki T. Purification and  
664 characterization of a novel type of fimbriae from the oral anaerobe *Bacteroides*  
665 *gingivalis*. *J Bacteriol.* 1984;160(3):949–957.
- 666 71. Yoshimura F, Watanabe K, Takasawa T, Kawanami M, Kato H. Purification and  
667 properties of a 75-kilodalton major protein, an immunodominant surface antigen,  
668 from the oral anaerobe *Bacteroides gingivalis*. *Infect Immun.* 1989;57(11):3646-  
669 3652.
- 670 72. Ogawa T, Yasuda K, Yamada K, Mori H, Ochiai K, Hasegawa M.  
671 Immunochemical characterisation and epitope mapping of a novel fimbrial protein  
672 (Pg-II fimbria) of *Porphyromonas gingivalis*. *FEMS Immunol Med Microbiol.*  
673 1995;11(3):247–255. doi:10.1111/j.1574-695X.1995.tb00122.x



- 674 73. Hamada N, Sojar HT, Cho MI, Genco RJ. Isolation and characterization of a  
675 minor fimbria from *Porphyromonas gingivalis*. *Infect Immun*. 1996;64(11):4788–  
676 4794.
- 677 74. Nagano K, Hasegawa Y, Yoshida Y, Yoshimura F. Novel fimbrilin PGN\_1808 in  
678 *Porphyromonas gingivalis*. *PLoS One*. 2017;12(3):e0173541. Published 2017 Mar  
679 15. doi:10.1371/journal.pone.0173541
- 680 75. Onoe T, Hoover CI, Nakayama K, Ideka T, Nakamura H, Yoshimura F.  
681 Identification of *Porphyromonas gingivalis* prefimbrilin possessing a long leader  
682 peptide: possible involvement of trypsin-like protease in fimbrilin maturation.  
683 *Microb Pathog*. 1995;19(5):351–364. doi:10.1016/s0882-4010(96)80006-4
- 684 76. Shoji M, Naito M, Yukitake H, et al. The major structural components of two cell  
685 surface filaments of *Porphyromonas gingivalis* are matured through lipoprotein  
686 precursors. *Mol Microbiol*. 2004;52(5):1513–1525. doi:10.1111/j.1365-  
687 2958.2004.04105.x
- 688 77. Hasegawa Y, Iwami J, Sato K, et al. Anchoring and length regulation of  
689 *Porphyromonas gingivalis* Mfa1 fimbriae by the downstream gene product Mfa2.  
690 *Microbiology*. 2009;155(Pt 10):3333–3347. doi:10.1099/mic.0.028928-0

- 691 78. Nagano K, Hasegawa Y, Murakami Y, Nishiyama S, Yoshimura F. FimB  
692 regulates FimA fimbriation in *Porphyromonas gingivalis*. *J Dent Res*.  
693 2010;89(9):903–908. doi:10.1177/0022034510370089
- 694 79. Nishiyama SI, Murakami Y, Nagata H, Shizukuishi S, Kawagishi I, Yoshimura F.  
695 Involvement of minor components associated with the FimA fimbriae of  
696 *Porphyromonas gingivalis* in adhesive functions. *Microbiology*. 2007;153(Pt  
697 6):1916–1925. doi:10.1099/mic.0.2006/005561-0
- 698 80. Hasegawa Y, Nagano K, Ikai R, et al. Localization and function of the accessory  
699 protein Mfa3 in *Porphyromonas gingivalis* Mfa1 fimbriae. *Mol Oral Microbiol*.  
700 2013;28(6):467–480. doi:10.1111/omi.12040
- 701 81. Ikai R, Hasegawa Y, Izumigawa M, et al. Mfa4, an accessory protein of Mfa1  
702 fimbriae, modulates fimbrial biogenesis, cell auto-aggregation, and biofilm  
703 formation in *Porphyromonas gingivalis*. *PLoS One*. 2015;10(10):e0139454.  
704 Published 2015 Oct 5. doi:10.1371/journal.pone.0139454
- 705 82. Hasegawa Y, Iijima Y, Persson K, et al. Role of Mfa5 in expression of Mfa1  
706 fimbriae in *Porphyromonas gingivalis*. *J Dent Res*. 2016;95(11):1291–1297.  
707 doi:10.1177/0022034516655083

- 708 83. Nelson KE, Fleischmann RD, DeBoy RT, et al. Complete genome sequence of the  
709 oral pathogenic Bacterium *Porphyromonas gingivalis* strain W83. *J Bacteriol.*  
710 2003;185(18):5591–5601. doi:10.1128/jb.185.18.5591-5601.2003
- 711 84. Naito M, Hirakawa H, Yamashita A, et al. Determination of the genome sequence  
712 of *Porphyromonas gingivalis* strain ATCC 33277 and genomic comparison with  
713 strain W83 revealed extensive genome rearrangements in *P. gingivalis*. *DNA Res.*  
714 2008;15(4): 215–225. doi:10.1093/dnares/dsn013
- 715 85. Kloppsteck P, Hall M, Hasegawa Y, Persson K. Structure of the fimbrial protein  
716 Mfa4 from *Porphyromonas gingivalis* in its precursor form: implications for a  
717 donor-strand complementation mechanism. *Sci Rep.* 2016;6:22945. Published  
718 2016 Mar 14. doi:10.1038/srep22945
- 719 86. Hall M, Hasegawa Y, Yoshimura F, Persson K. Structural and functional  
720 characterization of shaft, anchor, and tip proteins of the Mfa1 fimbria from the  
721 periodontal pathogen *Porphyromonas gingivalis*. *Sci Rep.* 2018;8(1):1793.  
722 Published 2018 Jan 29. doi:10.1038/s41598-018-20067-z
- 723 87. Alaei SR, Park JH, Walker SG, Thanassi DG. Peptide-based inhibitors of fimbrial  
724 biogenesis in *Porphyromonas gingivalis*. *Infect Immun.* 2019;87(3):e00750-18.  
725 Published 2019 Feb 21. doi:10.1128/IAI.00750-18

- 726 88. Shibata S, Shoji M, Okada K, et al. Structure of polymerized type V pilin reveals  
727 assembly mechanism involving protease-mediated strand exchange. *Nat*  
728 *Microbiol.* 2020; 5: 830-837. <https://doi.org/10.1038/s41564-020-0705-1>
- 729 89. Braun V, Wu HC. Lipoproteins: structure function, biosynthesis and model for  
730 protein export. *New Comp. Biochem.* 1994; 27, 319-341.
- 731 90. Yamagata H, Ippolito C, Inukai M, Inouye M. Temperature-sensitive processing  
732 of outer membrane lipoprotein in an *Escherichia coli* mutant. *J Bacteriol.*  
733 1982;152(3):1163–1168.
- 734 91. Petit CM, Brown JR, Ingraham K, Bryant AP, Holmes DJ. Lipid modification of  
735 prelipoproteins is dispensable for growth in vitro but essential for virulence in  
736 *Streptococcus pneumoniae*. *FEMS Microbiol Lett.* 2001;200(2):229–233.  
737 [doi:10.1111/j.1574-6968.2001.tb10720.x](https://doi.org/10.1111/j.1574-6968.2001.tb10720.x)
- 738 92. Réglie-Poupet H, Frehel C, Dubail I, et al. Maturation of lipoproteins by type II  
739 signal peptidase is required for phagosomal escape of *Listeria monocytogenes*. *J*  
740 *Biol Chem.* 2003;278(49):49469–49477. [doi:10.1074/jbc.M307953200](https://doi.org/10.1074/jbc.M307953200)
- 741 93. Armbruster KM, Meredith TC. Identification of the lyso-form *N*-acyl  
742 intramolecular transferase in low-GC Firmicutes. *J Bacteriol.*  
743 2017;199(11):e00099-17. Published 2017 May 9. [doi:10.1128/JB.00099-17](https://doi.org/10.1128/JB.00099-17)

- 744 94. Nakayama H, Kurokawa K, Lee BL. Lipoproteins in bacteria: structures and  
745 biosynthetic pathways. *FEBS J.* 2012;279(23):4247–4268.  
746 doi:10.1111/febs.12041
- 747 95. Hashimoto M, Asai Y, Ogawa T. Separation and structural analysis of lipoprotein  
748 in a lipopolysaccharide preparation from *Porphyromonas gingivalis*. *Int Immunol.*  
749 2004;16(10):1431–1437. doi:10.1093/intimm/dxh146
- 750 96. Matsuyama S, Tajima T, Tokuda H. A novel periplasmic carrier protein involved  
751 in the sorting and transport of *Escherichia coli* lipoproteins destined for the outer  
752 membrane. *EMBO J.* 1995;14(14):3365–3372.
- 753 97. Matsuyama Si, Yokota N, Tokuda H. A novel outer membrane lipoprotein, LolB  
754 (HemM), involved in the LolA (p20)-dependent localization of lipoproteins to the  
755 outer membrane of *Escherichia coli*. *EMBO J.* 1997;16(23):6947–6955.  
756 doi:10.1093/emboj/16.23.6947
- 757 98. Narita SI, Tokuda H. Bacterial lipoproteins; biogenesis, sorting and quality  
758 control. *Biochim Biophys Acta Mol Cell Biol Lipids.* 2017;1862(11):1414–1423.  
759 doi:10.1016/j.bbalip.2016.11.009
- 760 99. Takeda K, Miyatake H, Yokota N, Matsuyama S, Tokuda H, Miki K. Crystal  
761 structures of bacterial lipoprotein localization factors, LolA and LolB. *EMBO J.*

762 2003;22(13):3199–3209. doi:10.1093/emboj/cdg324

763 100.Tajima T, Yokota N, Matsuyama S, Tokuda H. Genetic analyses of the in vivo  
764 function of LolA, a periplasmic chaperone involved in the outer membrane  
765 localization of *Escherichia coli* lipoproteins. *FEBS Lett.* 1998;439(1-2):51–54.  
766 doi:10.1016/s0014-5793(98)01334-9

767 101.Fernández-Piñar R, Lo Sciuto A, Rossi A, Ranucci S, Bragonzi A, Imperi F. In  
768 vitro and in vivo screening for novel essential cell-envelope proteins in  
769 *Pseudomonas aeruginosa*. *Sci Rep.* 2015;5:17593. Published 2015 Dec 1.  
770 doi:10.1038/srep17593

771 102.Chalker AF, Minehart HW, Hughes NJ, et al. Systematic identification of selective  
772 essential genes in *Helicobacter pylori* by genome prioritization and allelic  
773 replacement mutagenesis. *J Bacteriol.* 2001;183(4):1259–1268.  
774 doi:10.1128/JB.183.4.1259-1268.2001

775 103.Rhodes RG, Samarasam MN, Van Groll EJ, McBride MJ. Mutations in  
776 *Flavobacterium johnsoniae sprE* result in defects in gliding motility and protein  
777 secretion. *J Bacteriol.* 2011;193(19):5322–5327. doi:10.1128/JB.05480-11

778 104.Zhu Y, McBride MJ. Comparative Analysis of *Cellulophaga algicola* and  
779 *Flavobacterium johnsoniae* Gliding Motility. *J Bacteriol.* 2016;198(12):1743–

780 1754. Published 2016 May 27. doi:10.1128/JB.01020-15

781 105.Liao CT, Chiang YC, Hsiao YM. Functional characterization and proteomic  
782 analysis of *lolA* in *Xanthomonas campestris* pv. *campestris*. *BMC Microbiol.*  
783 2019;19(1):20. Published 2019 Jan 21. doi:10.1186/s12866-019-1387-9

784 106.Grabowicz M, Silhavy TJ. Redefining the essential trafficking pathway for outer  
785 membrane lipoproteins. *Proc Natl Acad Sci U S A.* 2017;114(18):4769–4774.  
786 doi:10.1073/pnas.1702248114

787 107.Okuda S, Watanabe S, Tokuda H. A short helix in the C-terminal region of LolA is  
788 important for the specific membrane localization of lipoproteins. *FEBS Lett.*  
789 2008;582(15):2247–2251. doi:10.1016/j.febslet.2008.05.022

790 108.Hayashi Y, Tsurumizu R, Tsukahara J, et al. Roles of the protruding loop of factor  
791 B essential for the localization of lipoproteins (LolB) in the anchoring of bacterial  
792 triacylated proteins to the outer membrane. *J Biol Chem.* 2014;289(15):10530–  
793 10539. doi:10.1074/jbc.M113.539270

794 109.Sutcliffe IC, Harrington DJ, Hutchings MI. A phylum level analysis reveals  
795 lipoprotein biosynthesis to be a fundamental property of bacteria. *Protein Cell.*  
796 2012;3(3):163–170. doi:10.1007/s13238-012-2023-8

- 797 110. Webb CT, Heinz E, Lithgow T. Evolution of the  $\beta$ -barrel assembly machinery.  
798 *Trends Microbiol.* 2012;20(12):612–620. doi:10.1016/j.tim.2012.08.006
- 799 111. Klein BA, Tenorio EL, Lazinski DW, Camilli A, Duncan MJ, Hu LT.  
800 Identification of essential genes of the periodontal pathogen *Porphyromonas*  
801 *gingivalis*. *BMC Genomics.* 2012;13:578. Published 2012 Oct 31.  
802 doi:10.1186/1471-2164-13-578
- 803 112. Hutcherson JA, Gogeneni H, Yoder-Himes D, et al. Comparison of inherently  
804 essential genes of *Porphyromonas gingivalis* identified in two transposon-  
805 sequencing libraries. *Mol Oral Microbiol.* 2016;31(4):354–364.  
806 doi:10.1111/omi.12135
- 807 113. Levine TP. Remote homology searches identify bacterial homologues of  
808 eukaryotic lipid transfer proteins, including Chorein-N domains in TamB and  
809 AsmA and Mdm31p. *BMC Mol Cell Biol.* 2019;20(1):43. Published 2019 Oct 14.  
810 doi:10.1186/s12860-019-0226-z
- 811 114. Okuda S, Tokuda H. Lipoprotein sorting in bacteria. *Annu Rev Microbiol.*  
812 2011;65:239–259. doi:10.1146/annurev-micro-090110-102859
- 813 115. Konovalova A, Perlman DH, Cowles CE, Silhavy TJ. Transmembrane domain of  
814 surface-exposed outer membrane lipoprotein RcsF is threaded through the lumen



815 of  $\beta$ -barrel proteins. *Proc Natl Acad Sci U S A*. 2014;111(41):E4350–E4358.  
816 doi:10.1073/pnas.1417138111

817 116.Michel LV, Shaw J, MacPherson V, et al. Dual orientation of the outer membrane  
818 lipoprotein Pal in *Escherichia coli*. *Microbiology*. 2015;161(6):1251–1259.  
819 doi:10.1099/mic.0.000084

820 117.Schulze RJ, Zückert WR. *Borrelia burgdorferi* lipoproteins are secreted to the  
821 outer surface by default. *Mol Microbiol*. 2006;59(5):1473–1484.

822 118.Dowdell AS, Murphy MD, Azodi C, et al. Comprehensive Spatial Analysis of the  
823 *Borrelia burgdorferi* Lipoproteome Reveals a Compartmentalization Bias toward  
824 the Bacterial Surface. *J Bacteriol*. 2017;199(6):e00658-16. Published 2017 Feb  
825 28. doi:10.1128/JB.00658-16

826 119.Chen S, Zückert WR. Probing the *Borrelia burgdorferi* surface lipoprotein  
827 secretion pathway using a conditionally folding protein domain. *J Bacteriol*.  
828 2011;193(23):6724–6732. doi:10.1128/JB.06042-11

829 120.Kumru OS, Schulze RJ, Rodnin MV, Ladokhin AS, Zückert WR. Surface  
830 localization determinants of *Borrelia* OspC/Vsp family lipoproteins. *J Bacteriol*.  
831 2011;193(11):2814–2825. doi:10.1128/JB.00015-11

832 121.Zückert WR. Protein secretion in *Spirochetes*. *Microbiol Spectr*.

833 2019;7(3):10.1128/microbiolspec.PSIB-0026-2019.  
834 doi:10.1128/microbiolspec.PSIB-0026-2019

835 122.Anderson KL, Salyers AA. Biochemical evidence that starch breakdown by  
836 *Bacteroides thetaiotaomicron* involves outer membrane starch-binding sites and  
837 periplasmic starch-degrading enzymes. *J Bacteriol.* 1989;171(6):3192–3198.  
838 doi:10.1128/jb.171.6.3192-3198.1989

839 123.Wilson MM, Anderson DE, Bernstein HD. Analysis of the outer membrane  
840 proteome and secretome of *Bacteroides fragilis* reveals a multiplicity of secretion  
841 mechanisms. *PLoS One.* 2015;10(2):e0117732. Published 2015 Feb 6.  
842 doi:10.1371/journal.pone.0117732

843 124.Valguarnera E, Scott NE, Azimzadeh P, Feldman MF. Surface exposure and  
844 packing of lipoproteins into outer membrane vesicles are coupled processes in  
845 *Bacteroides. mSphere.* 2018 Nov 7;3(6). pii: e00559-18.  
846 doi:10.1128/mSphere.00559-18.

847 125.Lauber F, Cornelis GR, Renzi F. Identification of a new lipoprotein export signal  
848 in Gram-negative bacteria. *mBio.* 2016;7(5):e01232-16. Published 2016 Oct 25.  
849 doi:10.1128/mBio.01232-16

850 126.Berven FS, Karlsen OA, Straume AH, et al. Analysing the outer membrane

851 subproteome of *Methylococcus capsulatus* (Bath) using proteomics and novel  
852 biocomputing tools. *Arch Microbiol.* 2006;184(6):362–377. doi:10.1007/s00203-  
853 005-0055-7

854 127.Juncker AS, Willenbrock H, Von Heijne G, Brunak S, Nielsen H, Krogh A.  
855 Prediction of lipoprotein signal peptides in Gram-negative bacteria. *Protein Sci.*  
856 2003;12(8):1652–1662. doi:10.1110/ps.0303703

857 128.Gorasia DG, Veith PD, Hanssen EG, et al. Structural insights into the PorK and  
858 PorN components of the *Porphyromonas gingivalis* type IX secretion system.  
859 *PLoS Pathog.* 2016;12(8):e1005820. Published 2016 Aug 10.  
860 doi:10.1371/journal.ppat.1005820

861 129.Hooda Y, Lai CC, Judd A, et al. Slam is an outer membrane protein that is  
862 required for the surface display of lipidated virulence factors in *Neisseria*. *Nat*  
863 *Microbiol.* 2016;1:16009. Published 2016 Feb 29. doi:10.1038/nmicrobiol.2016.9

864 130.Hooda Y, Lai CCL, Moraes TF. Identification of a large family of Slam-dependent  
865 surface lipoproteins in Gram-negative bacteria. *Front Cell Infect Microbiol.*  
866 2017;7:207. Published 2017 May 31. doi:10.3389/fcimb.2017.00207

867

868 **Figure Legends**

869 **Fig. 1. N-terminal prosequences of FimA and Mfa1 proteins.**

870 Arginine residues of cleavage sites by Rgp are colored in red. Underlines indicate  
871 lipoprotein box signals.

872

873 **Fig. 2. Crystal structure of FimA protein.**

874

875 (A) Structure of FimA protein (FimA1) derived from strain ATCC 33277 (Protein Data  
876 Bank accession number: 6JZK), as observed using X-ray crystallography. FimA1 is  
877 composed of the N-terminal domain (NTD) and C-terminal domain (CTD). The arginine-  
878 specific cleavage site (R|A, in yellow) is marked by a scissor symbol. Mature protein  
879 begins at 47<sup>th</sup> alanine residue in the FimA amino acids. The conserved  $\beta$ -sheet core (cyan),  
880 the N-terminal anchor strand (blue), and the C-terminal donor strand (red) are colored.

881 (B) A topological diagram of a secondary structure of FimA1 color-coded as in (A).

882 Original figures are from Shibata et al. <sup>75</sup>.

883

884 **Fig. 3. Structure of FimA polymer.**

885

886 (A) An electron micrograph of negatively stained FimA polymers. A recombinant pro-  
887 FimA protein from strain ATCC 33277 was purified from *E. coli* and treated with RgpB  
888 protease purified from *P. gingivalis*, and subsequently formed a mixture of monomers  
889 and polymers of FimA. FimA polymers were precipitated using polyethylene glycol. The  
890 FimA polymers were negatively stained with uranyl acetate and imaged using electron  
891 microscopy. (B) Cryo-electron microscopic reconstruction. Single-particle cryo-electron  
892 microscopy analysis revealed the structure of the FimA polymer at the atomic level. The  
893 C-terminal donor strand of FimA acts as a linker sequence. Original figures are from  
894 Shibata et al.<sup>75</sup>.

895

896 **Fig. 4. Transport of Fim pilins and formation of Fim pili.**

897

898 The FimA protein (stalk pilin) is initially integrated into the inner membrane by the Sec  
899 apparatus. Signal sequence (orange), lipoprotein export signal (green), N-terminal anchor  
900 strand (blue), main body (cyan), and C-terminal donor strand (red) of FimA are indicated.  
901 The lipid-modified precursor form of FimA is transported from the inner membrane (IM)  
902 to the outer membrane (OM) via a putative ABC transporter and unknown factor(s). The  
903 lipid-modified precursor positioned at the cell surface is then cleaved by arginine-specific

904 proteases (Rgp) that are anchored to anionic lipopolysaccharide containing  
905 lipopolysaccharide (A-LPS) in the outer leaflet of the outer membrane, and subsequently  
906 form a mature FimA that consists of an outward C-terminal donor strand (red) and a  
907 hydrophobic groove partially occupied by the N-terminal anchor strand (blue). The N-  
908 terminal anchor strand embedded in the hydrophobic groove is not released immediately  
909 from the FimA main body even after it is cleaved by Rgp and plays a role in anchoring  
910 the FimA main body to the OM. Pilin polymerization is initiated upon the insertion of the  
911 C-terminal donor strand of an approaching FimA into the hydrophobic groove of the  
912 preceding FimA. The N-terminal anchor strand of the preceding FimA is released from  
913 the FimA main body upon the entry of the C-terminal donor strand of FimA. The reaction  
914 occurs continuously until the anchor pilin FimB is incorporated. Pilin polymerization at  
915 the cell surface may be initiated at the tip pilin that lacks the C-terminal donor strand. As  
916 the C-terminal donor strands are needed to form pili, it is unlikely that a tip pilin would  
917 be incorporated into a pilus at the filament tip after pilin polymerization. The stalk pilin  
918 FimA is sufficient for initiating pilus assembly *in vivo*; this indicates that initiation does  
919 not require a tip pilin, which would otherwise result in the formation of a mixed  
920 population of tipped and untipped pili.

921

922 **Fig. 5. Lipoprotein export sequence in *Porphyromonas gingivalis*.**

923

924 (A) The N-terminal lipid-modified cysteine and the subsequent amino acids of *P.*

925 *gingivalis* lipoproteins. The lipoproteins are classified based on their locations (outer

926 leaflet of the outer membrane, inner leaflet of the outer membrane, and unknown). (B)

927 Consensus lipoprotein export signals in surface lipoproteins of *Capnocytophaga*

928 *canimorsus*, *Flavobacterium johnsoniae*, and *Bacteroides fragilis*. Acidic amino acids

929 (green) and basic amino acids (cyan) are color-coded.

930

Fig. 1

FimA

MKKTKFFLLGLAALAMTACNKDNEAEPVTEGNATISVVLKTSNSN**RA**

Rgp



46 47

Mfa1

MKLNKMFLVGALLSLGFASCSKEGNGPDPD<sup>NA</sup>AKSYMSMTLSMPMGSA**RA**

Rgp

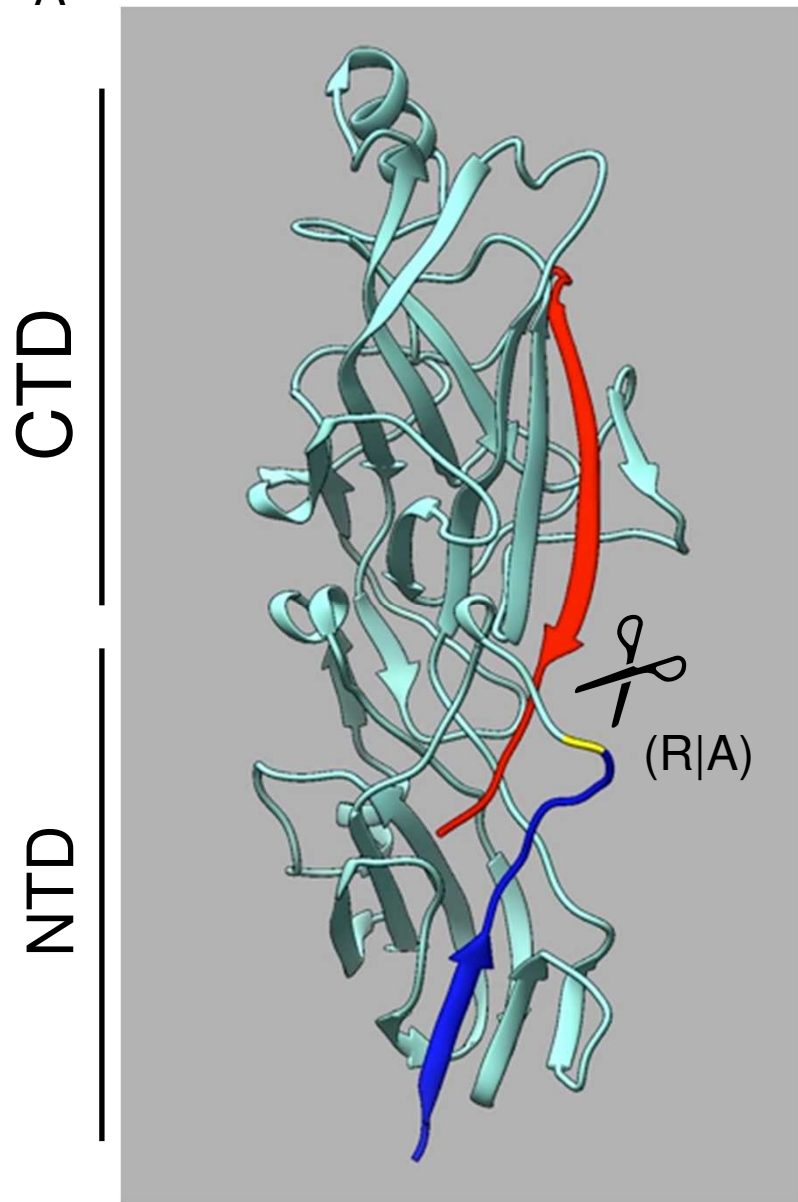


49 50



Fig. 2

A



B

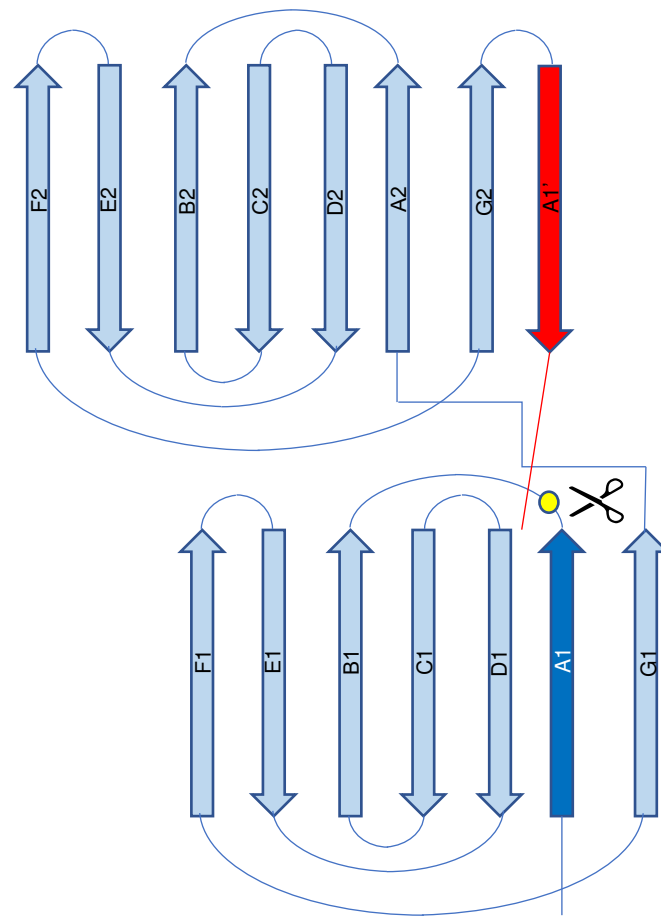
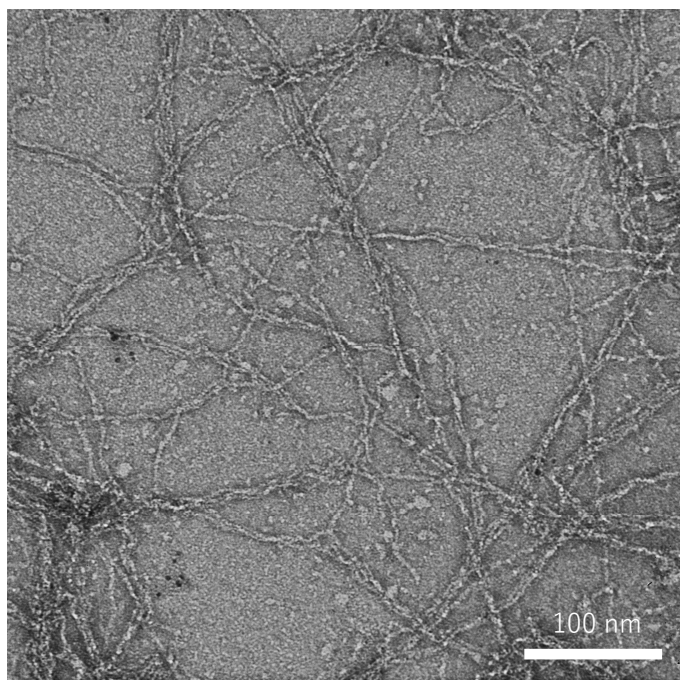


Fig. 3

A



B

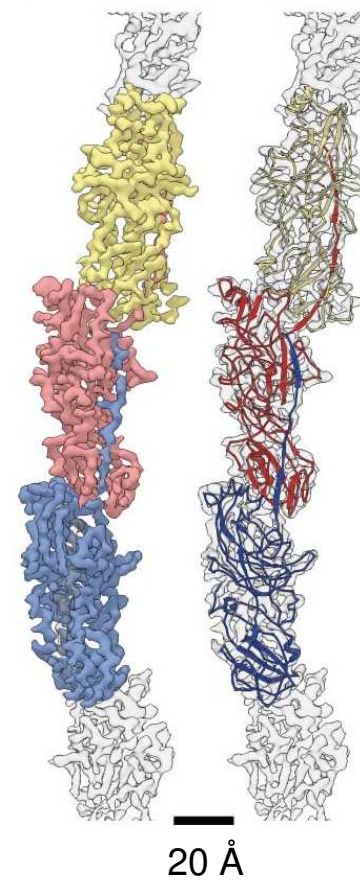


Fig. 4

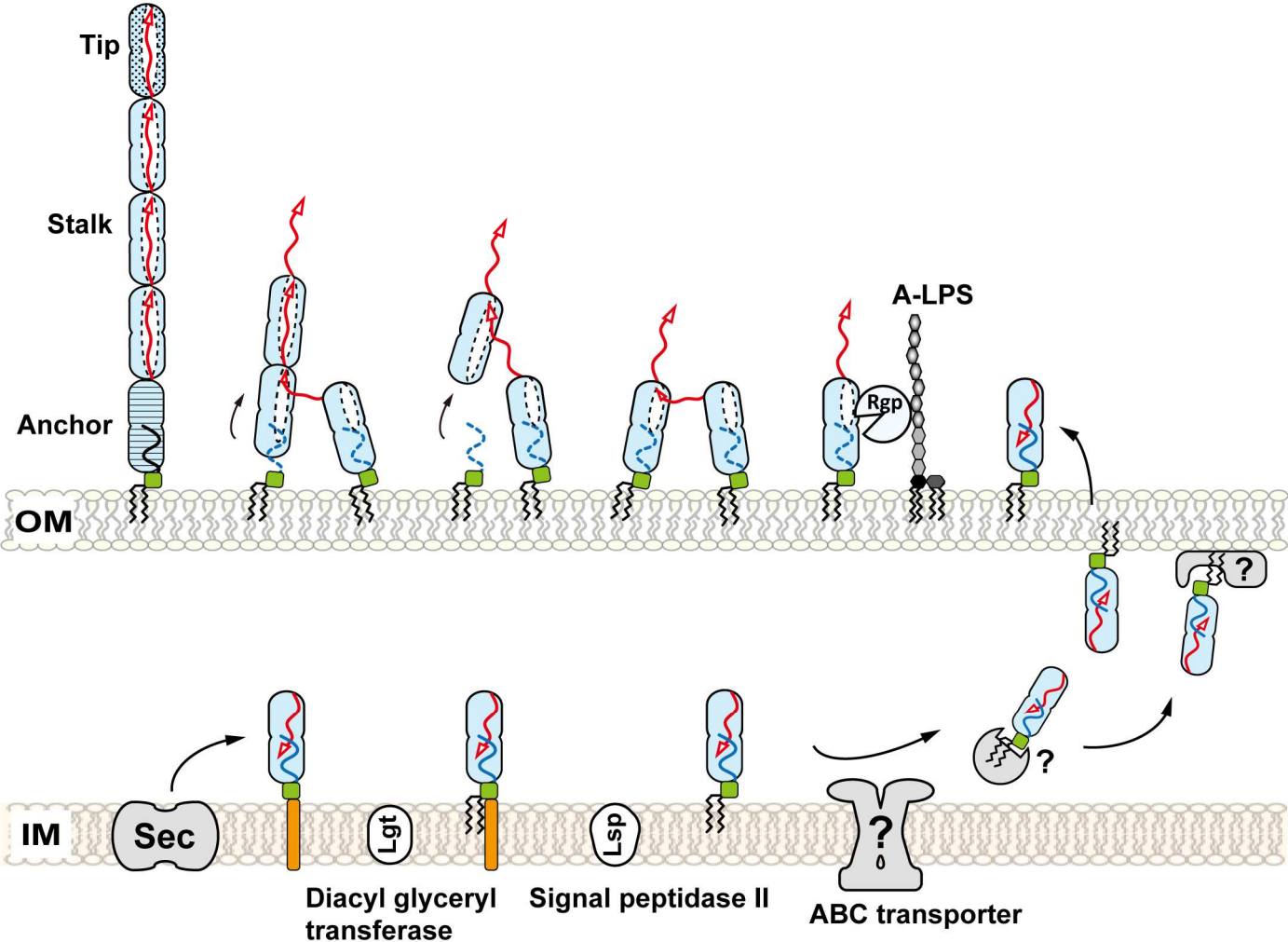


Fig. 5

